J. Fluid Mech. (1995), vol. 298, pp. 311–325

On the internal shear layers spawned by the critical regions in oscillatory Ekman boundary layers

By R. R. KERSWELL

Department of Mathematics and Statistics, University of Newcastle upon Tyne, Newcastle NE1 7RU, UK

(Received 21 July 1994 and in revised form 6 April 1995)

The Ekman boundary layer scalings associated with small oscillatory flows in a rapidly rotating system are well known to break down at the critical latitudes. The effect of these anomalous boundary regions on the interior flow has long been an issue of some concern. We argue, using analytical results derived in a model problem based on Stewartson's (1957) split-disk configuration, that these boundary regions spawn internal shear layers. These shear layers have their natural length scale of $E^{1/3}$ and carry velocities only $O(E^{1/6})$ smaller than the Rossby number – where E is the Ekman number – if the boundary is concave away from the fluid at the critical latitude. Otherwise, only a weaker shear layer is produced of length scale $E^{1/5}$ containing velocities of $O(E^{3/10})$ smaller than the Rossby number rather than the usual $O(E^{1/2})$ value for viscous flows in the interior. We show how these layers can carry angular momentum by themselves or more significantly in combination with the interior inviscid flow, so as to influence the mean flow at leading order. These conclusions are then discussed in the context of a precessing oblate spheroid of fluid for which detailed experimental observations are available.

1. Introduction

In the study of rapidly rotating viscous fluids, it has long become standard to assume that the effects of viscosity are largely confined to Ekman boundary layers, and that the solution both in the interior and in these boundary layers may be expanded in powers of $E^{1/2}$ (where E is the Ekman number defined below). As an exception to this, steady flows which additionally possess internal shear layers aligned with the axis of rotation have received considerable attention following the initial work by Morrison & Morgan (1956), Proudman (1956), and Stewartson (1957, 1966). Nestled layers of $E^{1/3}$, $E^{1/4}$ and even $E^{2/7}$ (Stewartson 1966) can be present to transport mass between the Ekman layers and resolve internal velocity discontinuities forced by the boundary conditions.

A similar but far less studied situation arises when the flow deviates slightly from its uniform rotation with an oscillation frequency λ less than twice the basic rotation rate ($-2 < \lambda < 2$). The relevant linearized inviscid equations are then hyperbolic and discontinuities may propagate without attenuation along the characteristic cones,

$$s \pm \frac{\lambda z}{(4-\lambda^2)^{1/2}} = \text{constant}, \tag{1.1}$$

where s is the cylindrical radius and z the axial coordinate, throughout the fluid. These discontinuities are naturally smoothed out in the presence of viscosity by internal shear layers established along the characteristic surfaces. Görtler (1944, 1957) and Oser

(1958) have observed these characteristic surfaces in a rotating suspension of aluminium powder, perturbed by an axially oscillating disk (see Greenspan 1968, figure 1.3 and §4.4 for a summary of the accompanying unbounded analysis by Morrison & Morgan 1956, Oser 1957 and Reynolds 1962*a*, *b*). Wood (1965, 1966) discussed the possibility of shear layers emanating out of the corner regions in his consideration of perturbations to a rotating cylinder of fluid. These were later experimentally observed by McEwan (1970). In a little known paper, Walton (1975*a*) considered the oscillatory analogue of Stewartson's (1957) steady split-disk problem, demonstrating that unsteady shear layers of thickness $E^{1/3}$ and exceptionally $E^{1/4}$ could be spawned by a discontinuity in the (viscous) boundary conditions. This work also served to emphasize the different wave-like natures of steady and oscillatory layers, with the former analogous to localized standing waves and the latter resembling propagating waves.

An outstanding issue in rotating fluids has then been whether the well-documented critical regions in oscillatory Ekman boundary layers may give rise to such shear layers penetrating into the interior (e.g. see Bondi & Lyttleton 1953; Greenspan 1968, p. 62; Vanyo *et al.* 1995). These critical regions, or boundary layer 'eruptions' as Bondi & Lyttleton christened them, represent a local breakdown in the Ekman layer scalings for the boundary layer associated with small inertial oscillations (Greenspan 1964, 1965, 1968) and occur at the critical latitude at which

$$2\hat{\boldsymbol{n}}\cdot\hat{\boldsymbol{k}} = \lambda, \tag{1.2}$$

where $\hat{\boldsymbol{n}}$ is the outward normal and $\hat{\boldsymbol{k}}$ the non-dimensionalized angular velocity of the container. At this latitude incoming energy carried by the inertial waves is reflected along the boundary instead of back into the interior (Phillips 1963; Greenspan 1968, p. 191). The effect is essentially inviscid and manifested in the structure of the inertial waves (Wood 1977, 1981; Kerswell 1994).

Roberts & Stewartson (1963) showed how the boundary layer may be rescaled at the critical latitudes to give an increased thickness of $O(E^{2/5})$ over a region of extent $O(E^{1/5})$†. This tended to suggest that the readjustment at the critical latitudes was localized and unintrusive into the interior. Furthermore, using these scalings, the contribution of the critical latitude regions to the viscous (complex) frequency correction experienced by the inertial wave was found to be negligible compared to that from the rest of the Ekman layer – experimental and numerical evidence appears to support this conclusion (Greenspan 1968, p. 66; Kerswell & Barenghi 1995; Hollerbach & Kerswell 1995). As a result, these critical areas have generally been considered dynamically unimportant. A notable exception to this was the work of Busse (1968) which addressed the mean flow generated within a precessing oblate spheroid. By retaining the critical latitude singularity in the leading boundary layer solution, he found that the nonlinearity in the boundary layer could drive a shear layer in the mean flow at the critical radius. Agreement with experiment appeared good (Malkus 1968, figure 3), suggesting that the critical regions clearly had an important effect on the interior mean flow.

With this in mind, it is the purpose of this paper to explore the direct effect of the critical latitude regions in the boundary layer on the interior flow. We argue that (i) the critical latitudes of an oscillatory Ekman layer *do* significantly affect the interior by spawning shear layers which penetrate into the bulk of the fluid and (ii) that these internal shear layers can transport angular momentum through the fluid either by

† If the tangential derivatives cannot be rescaled – when the extent of the boundary inclined at the critical angle is finite – Gans (1983) found that rescaled layers of thickness $O(E^{1/3})$ and $O(E^{1/4})$ could exist.

themselves or in concert with the prevailing inviscid interior flow. In other words, these boundary layer 'eruptions' can influence the mean flow across the entire bulk of the fluid through the obliquely inclined shear layers so spawned. These conclusions are based upon the realization that a boundary layer eruption effectively represents a region of rapid variation in the boundary conditions felt by the interior flow. As such it may be modelled by studying the effect of a localized signal of small wavelength on the viscous boundary conditions for a system which can be solved exactly – Stewartson's coaxial infinite disk configuration. Here exact solutions to the linearized equations of motion based upon a uniformly rotating state are formally available in terms of Hankel Transforms. These can then be evaluated asymptotically in the limit of small Ekman number to reveal the important features of the fluid response.

For clarity, we actually present the results summarized above in reverse order. It is first established that oscillatory shear layers produced by a discontinuity in the boundary conditions can carry angular momentum. Then, having developed the problem to consider shear layers spawned in more general circumstances, we argue that their total effect on the interior is little different from the discontinuous case. The detailed plan of the paper is as follows. Section 2 introduces the infinite coaxial split-disk system used previously by Stewartson (1957) and Walton (1975*a*) to study the effect of small discontinuities in the boundary conditions on the uniformly rotating interior. To extend these previous axisymmetric studies, we show how the Navier–Stokes equation admits separable asymmetric solutions in this cylindrical geometry. In §3, we impose a small asymmetric oscillatory differential motion of the inner disk relative to the outer disk and essentially recover the asymmetric analogue of Walton's oscillatory internal shear layer solution. This solution is then used in §4 to establish that these shear layers exert a torque on the interior and hence can carry angular momentum away from the discontinuity. Although this is a somewhat idealized calculation, the implication is clear: these shear layers present a new source of Reynolds stresses whether viewed purely as a self-interaction or in combination with the leading interior inviscid flow. In the latter case, these stresses certainly would seem to be influential in determining the leading-order mean flow.

In §5, we consider the continuous analogue of the split-disk problem in which the adjustment in motion between the inner and outer disks is now smoothly achieved over a small length scale δ. This is a crude model of the critical region of a boundary layer in the sense that this area of readjustment represents a localized signal of some length scale δ in the boundary layer. At the boundary layer eruption, two characteristic directions are generally available to accommodate a shear layer: one directed back into the fluid and the other tangential to the boundary (with both inclined at $\tan^{-1}\lambda/(4-\lambda^2)^{1/2}$ to the rotation axis). For the non-tangential shear layer, the appropriate length scale would appear to be $E^{1/5}$, i.e. the shear layer sees the whole lateral extent of the eruption. On the other hand, the tangential shear layer sees only the boundary layer thickness change of $O(E^{2/5})$. The picture which emerges from the model is that *any* small-scale variation in the boundary layer is sufficient to generate internal shear layers. The strength of these shear layers is found to scale inversely with their lateral extent δ, until the natural scaling found by Walton is reached at $\delta \sim E^{1/3}$. In this way, their cumulative effect on the interior is equivalent to the discontinuous or $\delta \ll E^{1/3}$ case. The conclusions drawn in the latter idealized case in §4 are then more generally applicable.

The conclusions of the paper are brought together in §6 along with a brief discussion of their implications for a rotating system of current interest: the flow within a precessing oblate spheroid. Finally, an Appendix discusses the special resonant case of the oscillating disk problem in which the frequency of oscillation is exactly twice the rotation rate. In this limiting situation, the whole boundary is at the critical latitude.

2. The coaxial disk system

The coaxial disk system consists of an incompressible fluid contained between two infinite horizontal disks at $z = \pm d$ corotating with an angular velocity $\hat{\boldsymbol{k}}$ perpendicular to their plane. By dividing these disks into an inner and outer disk and imparting a small differential motion between the two, both Stewartson (1957) and Walton (1975*a*) have been able to study the effect of discontinuities in the boundary conditions on the uniformly rotating interior. In particular, Walton considered one of the outer disks to have a small additional oscillatory angular velocity $\epsilon\hat{\boldsymbol{k}}\exp(\mathrm{i}\lambda t)$ and concentrated on understanding the intricate pattern of reflecting internal shear layers produced. The attraction of the unbounded disk configuration is that the Navier–Stokes equation is separable in cylindrical polar coordinates (s, ϕ, z). Working in Cartesian coordinates and using the inner disk radius and basic rotation rate to non-dimensionalize the system, the linearized momentum equation describing small incompressible motions superimposed upon a uniformly rotating underlying state,

$$\frac{\partial \boldsymbol{u}}{\partial t} + 2\hat{\boldsymbol{k}} \times \boldsymbol{u} + \boldsymbol{\nabla} p = E\nabla^2 \boldsymbol{u}, \tag{2.1}$$

can be rewritten $\boldsymbol{\nabla}\cdot\boldsymbol{u} = 0$ as the three scalar equations

$$2\left[\frac{\partial u_y}{\partial x} - \frac{\partial u_x}{\partial y}\right] = \nabla^2 p, \tag{2.2}$$

$$\left(\frac{\partial}{\partial t} - E\nabla^2\right)\left[\frac{\partial u_y}{\partial x} - \frac{\partial u_x}{\partial y}\right] = 2\frac{\partial u_z}{\partial z}, \tag{2.3}$$

$$\left(\frac{\partial}{\partial t} - E\nabla^2\right) u_z = -\frac{\partial p}{\partial z}. \tag{2.4}$$

These can then be simplified to

$$\mathscr{L}[p] = \mathscr{L}[u_z] = 0, \quad \left\{\left(\frac{\partial}{\partial t} - E\frac{\partial^2}{\partial z^2}\right)^2 + 4\right\}\mathscr{L}[u_x \pm \mathrm{i}u_y] = 0, \tag{2.5}$$

where

$$\mathscr{L} = \left(\frac{\partial}{\partial t} - E\nabla^2\right)^2 \nabla^2 + 4\frac{\partial^2}{\partial z^2}. \tag{2.6}$$

Moving to cylindrical polar coordinates,

$$u_x \pm \mathrm{i}u_y = [U \pm \mathrm{i}V]\,\mathrm{e}^{\pm \mathrm{i}\phi}, \quad u_z = W \tag{2.7}$$

and separating variables

$$\boldsymbol{u}(\boldsymbol{x}, t) = [u(\boldsymbol{x}, t)\,\hat{\boldsymbol{s}} + v(\boldsymbol{x}, t)\,\hat{\boldsymbol{\phi}} + w(\boldsymbol{x}, t)\,\hat{\boldsymbol{z}}] = [U(s)\,\hat{\boldsymbol{s}} + V(s)\,\hat{\boldsymbol{\phi}} + W(s)\,\hat{\boldsymbol{z}}]\,\mathrm{e}^{\mathrm{i}(\lambda t + m\phi + \alpha z)}, \tag{2.8}$$

we find the solutions

$$U \pm \mathrm{i}V = \frac{\mathrm{i}\lambda - E(\alpha^2 - k^2)}{\mathrm{i}(\lambda \pm 2) - E(\alpha^2 - k^2)}\left(\mp\frac{k}{\alpha}\right) J_{m\pm 1}(ks), \tag{2.9}$$

$$W = J_m(ks), \tag{2.10}$$

provided that
$$[E(\alpha^2-k^2)-\mathrm{i}\lambda]^2(\alpha^2-k^2)+4\alpha^2 = 0. \tag{2.11}$$

The general solution is then a linear superposition of these:

$$u\pm \mathrm{i}v = \epsilon \sum_{m=-\infty}^{\infty}\sum_{l=1}^{3}\int_0^\infty \mathrm{d}k\, \frac{\mathrm{i}\lambda-E(\alpha_l^2-k^2)}{\mathrm{i}(\lambda\pm 2)-E(\alpha_l^2-k^2)}\left(\mp\frac{k}{\alpha_l}\right)A_l(k)\,J_{m\pm 1}(ks)\cosh(\alpha_l z)\,\mathrm{e}^{\mathrm{i}(\lambda t+m\phi)}, \tag{2.12}$$

$$w = \epsilon \sum_{m=-\infty}^{\infty}\sum_{l=1}^{3}\int_0^\infty \mathrm{d}k\, A_l(k)\,J_m(ks)\sinh(\alpha_l z)\,\mathrm{e}^{\mathrm{i}(\lambda t+m\phi)}, \tag{2.13}$$

where the subscript l runs over the three roots of (2.11) for each value of k. For convenience and without loss of generality, we have assumed symmetry about the mid-plane; in contrast to Stewartson's steady situation there is no fundamental difference between symmetric and antisymmetric solutions as the discontinuities vertically displaced in the upper and lower disks cannot communicate with each other.

3. Discontinuous boundary conditions

The main motivation behind this study is to consider the Ekman boundary layers associated with asymmetric inertial waves: specifically, the $m = 1$ case is of particular relevance to the precessing flows discussed in §6. As a result we will consider the inner disk to possess a small differential *asymmetric* motion relative to the outer disk. In practice, this could be achieved by arranging for a sector of the inner disk to rotate differentially compared to the rest of the system, thereby setting up discontinuities in the boundary conditions with respect to both ϕ and s. The discontinuities in ϕ may be Fourier decomposed into a full spectrum of azimuthal wavenumbers, each of which can then be considered separately due to the linearity of the system. By focusing on one such azimuthal mode m, we can then concentrate upon the effect of an asymmetric boundary condition discontinuity in s on the interior.

For our purpose, which is to discuss interior velocity fields larger than $O(\epsilon E^{1/2})$, the exact s-dependence of the boundary conditions away from the discontinuity is in fact irrelevant providing that their scale of variation remains $O(1)$. As a result, we are free to choose this to facilitate the analysis as Stewartson (1957) did. Furthermore, we impose $u+\mathrm{i}v = w = 0$ on the differentially rotating inner disk rather than the more natural $u = w = 0$ purely to exploit an exact inverse Hankel transform. The following analysis is insensitive to the imposed phase or amplitude relationship between u and v at the boundary and hence the results obtained below for the former case are then entirely representative of those corresponding to the latter. What is important is that the boundary conditions can only be viscously transmitted to the interior, i.e. $w = 0$ on the inner disk. With this in mind, we allow the inner disk to possess the rather artificial asymmetric differential motion

$$\boldsymbol{u} = [u,v,w] = \begin{cases} \epsilon[-\mathrm{i},1,0]\,s^{m-1}\,\mathrm{e}^{\mathrm{i}(\lambda t+m\phi)}, & s<1 \\ \boldsymbol{0}, & s>1 \end{cases} \tag{3.1}$$

at $z=\pm d$ relative to the outer disk so that with the identity

$$\int_0^\infty J_m(k)\,J_{m-1}(ks)\,\mathrm{d}k = \begin{cases} s^{m-1}, & 0<s<1 \\ 1/2, & s=1 \\ 0, & s>1 \end{cases} \tag{3.2}$$

(Sneddon 1951, p. 51), the boundary conditions then become simply

$$\sum_{l=1}^{3} \frac{\mathrm{i}\lambda - E(\alpha_l^2-k^2)}{\mathrm{i}(\lambda \pm 2) - E(\alpha_l^2-k^2)}\left(\frac{k}{\alpha_l}\right) A_l(k)\cosh(\alpha_l d) = \begin{cases} 0 & \text{(upper sign)} \\ -2\mathrm{i}J_m(k) & \text{(lower sign)}, \end{cases} \quad (3.3)$$

$$\sum_{l=1}^{3} A_l \sinh(\alpha_l d) = 0. \quad (3.4)$$

Away from the disk surfaces outside the Ekman layers, the only radial wavenumbers which contribute in the integrals of (2.12)–(3.4) satisfy $k \ll E^{-1/2}$, i.e. the smallest scales which exist in the interior are much larger than $E^{1/2}$. This is crucial for making progress for then the roots of (2.11) can be identified as follows:

$$\alpha_1 = \frac{\mathrm{i}k\lambda}{(4-\lambda^2)^{1/2}} + \frac{16k^3 E}{(4-\lambda^2)^{5/2}} + O(E^2 k^5), \quad (3.5)$$

$$\left.\begin{matrix}\alpha_2^2 \\ \alpha_3^2\end{matrix}\right\} = \frac{\mathrm{i}(\lambda \pm 2)}{E} + k^2\left[\frac{\lambda \pm 3}{\lambda \pm 2}\right] + O(E^2 k^4). \quad (3.6)$$

The special resonant case $\lambda = 2$ is considered in the Appendix. The roots α_2 and α_3, and hence the coefficients A_2 and A_3 correspond to the Ekman layer solutions which decay exponentially into the interior. If we focus our attention on the interior, only the solution given by A_1 is important and from the boundary conditions this is

$$A_1 \approx -E^{1/2}\frac{[\mathrm{i}(\lambda-2)]^{1/2}}{2-\lambda}\frac{kJ_m(k)}{\sinh(\alpha_1 d)} \quad (3.7)$$

to leading order, which will prove sufficient.

At this point we may proceed to evaluate the integrals (2.12) and (2.13) by contour integration as Stewartson (1957) originally did for his. More useful, however, is to realize that the integrands are only significant at large k values. This allows the integrand to be treated asymptotically and reveals more readily the individual shear layers and their reflections on the disks and in the axis (Walton 1975*a*). As

$$kJ_m(k)\,J_{m\pm 1}(ks) \sim \mp\frac{1}{2\pi s^{1/2}}\{(-1)^m \mathrm{e}^{\mathrm{i}k(s+1)} + \mathrm{i}\,\mathrm{e}^{\mathrm{i}k(s-1)} + \text{c.c.}\}, \quad (3.8)$$

$$\frac{\cosh(\alpha_1 z)}{\sinh(\alpha_1 d)} \sim \{\mathrm{e}^{\alpha_1(z-d)} + \mathrm{e}^{-\alpha_1(z+d)}\}\sum_{n=0}^{\infty} \mathrm{e}^{-2n\alpha_1 d}, \quad (3.9)$$

and defining $\gamma = \lambda/(4-\lambda^2)^{1/2}$ such that

$$\alpha_1 = \mathrm{i}k\gamma + \frac{16k^3 E}{(4-\lambda^2)^{5/2}} + O(k^5 E^2), \quad (3.10)$$

then

$$\begin{aligned} u \pm \mathrm{i}v \sim -\frac{\epsilon E^{1/2}}{2\pi s^{1/2}} \sum_{n=0}^{\infty} \int_0^{\infty} \mathrm{d}k \frac{\mathrm{i}\lambda - E(\alpha_1^2-k^2)}{\mathrm{i}(\lambda \pm 2) - E(\alpha_1^2-k^2)}\left(\frac{k[\mathrm{i}(\lambda-2)]^{1/2}}{\alpha_1(2-\lambda)}\right) \\ \times\{\mathrm{i}(\mathscr{F}[s-1,(1+2n)d-z] - \mathscr{F}[1-s,(1+2n)d-z] \\ + \mathscr{F}[s-1,(1+2n)d+z] - \mathscr{F}[1-s,(1+2n)d+z]) \\ +(-1)^m(\mathscr{F}[s+1,(1+2n)d-z] + \mathscr{F}[-s-1,(1+2n)d-z] \\ + \mathscr{F}[s+1,(1+2n)d+z] + \mathscr{F}[-s-1,(1+2n)d+z])\}\,\mathrm{e}^{\mathrm{i}(\lambda t + m\phi)}, \end{aligned} \quad (3.11)$$

where

$$\mathscr{F}[x,y] = \exp[\mathrm{i}k(x-\gamma y) - 16k^3 Ey/(4-\lambda^2)^{5/2}]. \tag{3.12}$$

The shear layer structure of the solution is encapsulated in the functions $\mathscr{F}[x,y]$. If $x-\gamma y$ is $O(1)$, then even though $\mathscr{F}$ is significant to $k = O(E^{-1/3})$, its rapid oscillation ensures that any integral of it remains $O(1)$ and hence $u \pm \mathrm{i}v = O(E^{1/2})$. However, in the shear layer (inclined at $\tan^{-1}\lambda/(4-\lambda^2)^{1/2}$ to the rotation axis) where $x-\gamma y$ is $O(E^{1/3})$, there is no such oscillation and $u \pm \mathrm{i}v$ is then $O(E^{1/6})$. It is also clear that the decay in the velocity magnitudes away from the shear layers can only be algebraic as Walton pointed out. The first four terms represent the original shear layers emanating from $s = 1$, $z = \pm d$ ($n = 0$) and their subsequent reflections ($n \neq 0$). The last four terms are the 'image' shear layers originating from the 'image' points $s = -1$, $z = \pm d$, and their reflections.

4. Angular momentum transfer

To identify the angular momentum transport of these shear layers through the interior, we consider the torque $T(s)$ exerted by the shear layer velocity field through its Reynolds stress on a cylinder of radius s. The component tending to despin the interior is

$$-\boldsymbol{T}\cdot\hat{\boldsymbol{k}} = T(s) = -\int_0^{2\pi}\int_{-d}^{d} s\,\mathrm{d}\phi\,\mathrm{d}z\,\hat{\boldsymbol{k}}\cdot\boldsymbol{r}\times\boldsymbol{u}\cdot\nabla\boldsymbol{u} = -\int_{-d}^{d}\mathrm{d}z\frac{\partial}{\partial s}\left(s^2\int_0^{2\pi} uv\,\mathrm{d}\phi\right). \tag{4.1}$$

Owing to the azimuthal integration, the product uv is time-averaged and therefore components of u and v which are $\frac{1}{2}\pi$ out of phase cannot contribute to the torque. Expression (3.11) shows that this is the case to leading order in Ek^2. Working to next order and away from shear layer intersections, the torque is produced entirely by the self-interaction of each shear layer velocity field. We therefore focus upon the angular momentum carried by one such shear layer which propagates inwards from the top discontinuity. Dropping $O(1)$ amplitudes and a common phase,

$$\left.\begin{aligned} u &\sim \frac{\epsilon E^{1/2}}{s^{1/2}}\mathrm{e}^{\mathrm{i}(\lambda t+m\phi)}\int_0^\infty \mathrm{d}k\left\{\frac{\mathrm{i}\lambda^2}{4-\lambda^2} - \frac{32Ek^2\lambda}{(4-\lambda^2)^3}\right\}\mathscr{F}[1-s, d-z],\\ v &\sim \frac{\epsilon E^{1/2}}{s^{1/2}}\mathrm{e}^{\mathrm{i}(\lambda t+m\phi)}\int_0^\infty \mathrm{d}k\left\{\frac{2\lambda}{4-\lambda^2} + \frac{8\mathrm{i}Ek^2(\lambda^2+4)}{(4-\lambda^2)^3}\right\}\mathscr{F}[1-s, d-z].\end{aligned}\right\} \tag{4.2}$$

Then using the real parts only, we have

$$T(s) = \frac{4\pi\lambda^2\epsilon^2E^2}{(4-\lambda^2)^3}\int_{-d}^{d}\mathrm{d}z\frac{\partial}{\partial s}s\int_0^\infty\int_0^\infty \mathrm{d}k_1\,\mathrm{d}k_2(k_1^2+k_2^2)\cos\{(k_1-k_2)[1-s-\gamma(d-z)]\}$$
$$\times\exp\left[-\frac{16E(k_1^3+k_2^3)(d-z)}{(4-\lambda^2)^{5/2}}\right]. \tag{4.3}$$

The change of variables

$$\xi = k_1 - k_2, \quad \eta = k_1^3 + k_2^3 \tag{4.4}$$

allows one integration to be completed immediately:

$$T(s) = \frac{\pi\lambda^2\epsilon^2E}{6(4-\lambda^2)^{1/2}}\frac{\partial}{\partial s}s\left\{\mathrm{Re}\int_-^+\frac{\mathrm{d}z}{d-z}\int_0^\infty \mathrm{d}\xi\exp\left[\mathrm{i}\xi[1-s-\gamma(d-z)] - \frac{16E(d-z)}{(4-\lambda^2)^{5/2}}\xi^3\right]\right\}. \tag{4.5}$$

Here we label the limits on the z-integration as merely $+$ and $-$ to indicate that the integration is taken across the shear layer. Working with the shear layer variables

$$X = \frac{1-s-\gamma(d-z)}{E^{1/3}}, \quad \tau = E^{1/3}\xi \tag{4.6}$$

the despinning torque may be rewritten as

$$T(s) = \frac{\pi\lambda^2\epsilon^2 E}{6(4-\lambda^2)^{1/2}}\frac{\partial}{\partial s}s\int_{-O(E^{-1/3})}^{+O(E^{-1/3})} \mathrm{d}X \int_0^\infty \frac{\mathrm{d}\tau}{1-s-E^{1/3}X}\exp\left[\mathrm{i}X\tau - \frac{16(1-s-E^{1/3}X)}{\gamma(4-\lambda^2)^{5/2}}\tau^3\right]. \tag{4.7}$$

The integrand is significant only when $X = O(1)$, that is inside the shear layer, and so the $E^{1/3}X$ terms may be dropped to leading order. Extending the limits of X to $\pm\infty$ with negligible error gives a δ-function in τ for the X-integration and then simply

$$T(s) \sim \left(\frac{\pi^2\lambda^2}{6(4-\lambda^2)^{1/2}}\right)\frac{\epsilon^2 E}{(1-s)^2}. \tag{4.8}$$

We might reasonably have anticipated a despinning torque of $O(\epsilon^2 E^{2/3})$ produced by the $O(\epsilon E^{1/6})$ velocity fields $\boldsymbol{u}_s$ interacting over the shear layer width $O(E^{1/3})$. However, the torque is reduced by a further factor of $O(E^{1/3})$ due to the phase incoherence between u and v in the shear layer. Such a torque will only drive an $O(\epsilon^2 E^{1/2})$ mean flow in the interior compared to the $O(\epsilon^2)$ mean flow produced by nonlinearities in the Ekman boundary layer.

In the full system of which this is just a model, there would of course be the inertial wave flow $\boldsymbol{u}_0$ present in the interior. This, working in tandem with the internal shear layer $\boldsymbol{u}_s$, would yield a despinning torque on the interior of

$$-\boldsymbol{T}\cdot\hat{\boldsymbol{k}} = -\int_0^{2\pi}\int_{-d}^{d} s\,\mathrm{d}\phi\,\mathrm{d}z\,\hat{\boldsymbol{k}}\cdot\boldsymbol{r}\times(\boldsymbol{u}_s\cdot\nabla\boldsymbol{u}_0+\boldsymbol{u}_0\cdot\nabla\boldsymbol{u}_s). \tag{4.9}$$

The second term in the integrand is of $O(\epsilon\times E^{-1/3}\times\epsilon E^{1/6})$ due to the normal derivative of the shear layer velocity. But, rather than driving an $O(\epsilon^2 E^{-1/3})$ mean flow, this leading-order effect vanishes under integration across the layer. However, that these large localized stresses are possible at all in such a generic way is extremely noteworthy. As far as the mean flow is concerned, this leaves both terms of the integrand to give an effect of $O(\epsilon\times\epsilon E^{1/6}\times E^{1/3} = \epsilon^2 E^{1/2})$ and hence be capable of driving the usual $O(\epsilon^2)$ mean flow. In contrast to the self-interaction of a shear layer, phase incoherence will not reduce this estimate because the shear layer is viscously generated and hence phase-lagged to the original inviscid interior flow.

It is worth emphasizing at this point that there is no net mass transport along the shear layer owing to its oscillatory nature. This said, the mass flux is $O(\epsilon E^{1/2})$ at a given instant in time and hence comparable to the general viscous flows in the interior.

5. Boundary layer eruptions

We now generalize the above by smoothing the discontinuity over a length scale δ. If the boundary is convex into the fluid at the critical latitude, only one shear layer orientation is possible pointed directly back into the fluid. Adopting the scalings of Roberts & Stewartson (1963), this shear layer sees an anomaly region of extent $O(E^{1/5}) \gg O(E^{1/3})$. Alternatively, if the boundary is concave into the fluid at the critical latitude, an additional shear layer is possible tangential to the boundary. This shear layer sees the anomalous boundary layer thickness of $O(E^{2/5}) \ll O(E^{1/3})$. Ostensibly, these appear completely different situations given the natural $E^{1/3}$ scalings of the shear layers discussed above. However, it is our purpose in this section to demonstrate that the shear layer scalings adjust themselves to accommodate *any* boundary variation scale once this exceeds $O(E^{1/3})$.

We consider the smoothed analogue of the inner disk moving differentially from the outer disk studied in §3. The small length scale δ controls the width of our 'boundary layer eruption' modelled by the boundary conditions

$$\boldsymbol{u} = \epsilon[-\mathrm{i}, 1, 0]\, s^{m-1} \frac{1}{\delta\pi^{1/2}} \int_s^\infty \epsilon^{-(y-1)^2/\delta^2}\, \mathrm{d}y\, \mathrm{e}^{\mathrm{i}(\lambda t + m\phi)} \tag{5.1}$$

at $z = \pm d$. In keeping with our knowledge of the boundary layer eruption, only the velocity gradients and not the velocities themselves are rescaled. The analysis presented in §3 can be reused for $\delta \neq 0$ provided that the Hankel transform $J_m(k)$ is replaced by

$$\frac{1}{\delta\pi^{1/2}} \int_0^\infty \mathrm{d}x\, x^m J_m(kx)\, \mathrm{e}^{-(x-1)^2/\delta^2} \tag{5.2}$$

in (3.3) and (3.7). Then, away from the Ekman boundary layers, the vertical velocity, for instance, is

$$w \sim -\epsilon E^{1/2} \frac{[\mathrm{i}(\lambda-2)]^{1/2}}{2-\lambda} \mathrm{e}^{\mathrm{i}(\lambda t + m\phi)} \int_0^\infty \int_0^\infty \mathrm{d}k\, \mathrm{d}x \frac{1}{\delta\pi^{1/2}} k x^m J_m(kx) J_m(ks)\, \mathrm{e}^{-(x-1)^2/\delta^2} \frac{\sinh(\alpha_1 z)}{\sinh(\alpha_1 d)}. \tag{5.3}$$

The integrand is significant only for $x - 1 = O(\delta)$ and for large k. Expanding the integrand asymptotically as before but this time retaining just the shear layer emanating directly out of the region towards the axis, gives

$$w \sim -\epsilon E^{1/2} \frac{[\mathrm{i}(\lambda-2)]^{1/2}}{2\pi(2-\lambda)\, s^{1/2}} \mathrm{e}^{\mathrm{i}(\lambda t + m\phi)} \int_0^\infty \mathrm{d}k\, \mathscr{F}[1-s, d-z] \int_0^\infty \frac{x^{m-1/2}\,\mathrm{d}x}{\delta\pi^{1/2}} \mathrm{e}^{\mathrm{i}k(x-1)-(x-1)^2/\delta^2}. \tag{5.4}$$

Rescaling the inner integral using $X\delta = x - 1$, extending the lower limit to $-\infty$ and setting $x^{m-1/2} \approx 1$ transforms this integral with negligible error into the Fourier transform of $\exp[-X^2]$ with respect to $k\delta$, i.e.

$$\int_0^\infty \frac{x^{m-1/2}\,\mathrm{d}x}{\delta\pi^{1/2}} \mathrm{e}^{\mathrm{i}k(x-1)-(x-1)^2/\delta^2} \sim \frac{1}{\pi^{1/2}} \int_{-\infty}^{+\infty} \mathrm{d}X\, \mathrm{e}^{\mathrm{i}(k\delta)X - X^2} = \mathrm{e}^{-k^2\delta^2/4}. \tag{5.5}$$

Hence

$$w \sim -\epsilon E^{1/2} \frac{[\mathrm{i}(\lambda-2)]^{1/2}}{2\pi(2-\lambda)\, s^{1/2}} \mathrm{e}^{\mathrm{i}(\lambda t + m\phi)} \times \int_0^\infty \mathrm{d}k \exp[\mathrm{i}k[1 - s + \gamma(z-d)] - k^2\delta^2/4 - 16k^3 E(d-z)/(4-\lambda^2)^{5/2}]. \tag{5.6}$$

The integrand is then significant up to

$$k \sim O[\min(1/\delta, E^{-1/3})] \gg 1, \tag{5.7}$$

and correspondingly within the shear layer

$$1-s+\gamma(z-d) = O[\max(\delta, E^{1/3})] \tag{5.8}$$

the vertical velocity will be

$$w = O[\min(\epsilon E^{1/2}/\delta, \epsilon E^{1/6})] \quad \text{or} \quad O[\min(1/\delta, E^{-1/3})] \gg 1 \tag{5.9}$$

larger than outside the shear layer. Thus, regardless of the exact small scaling δ, the interior feels the presence of the fine boundary layer variation through the production of suitably scaled shear layers directed along the characteristic directions. Such propagation of a 'signal' in the boundary conditions is, of course, typical of a hyperbolic system.

Thinking specifically in terms of the boundary layer eruptions and taking $\delta = E^{1/5}$, we can expect a shear layer of width $O(E^{1/5})$ to emerge in which the velocities are $O(\epsilon E^{3/10})$, that is, $O(E^{-1/5})$ larger than in the general interior. If the scale of variation is smaller than $E^{1/3}$, the $E^{1/3}$ shear layer formed does not see the fine structure but rather only a discontinuity in the boundary layer. This latter result has been assumed previously to match Stewartson shear layers to Ekman boundary layers (Greenspan & Howard 1963; Jacobs 1964; Stewartson 1966; Moore & Saffman 1969). Therefore, the shear layer tangential to the boundary layer eruption sensing only a $O(E^{2/5})$ thickness variation will have the 'maximum' strength of an $E^{1/3}$ layer, carrying $O(\epsilon E^{1/6})$ velocities.

The torque exerted on the interior by shear layers of width δ acting on their own or in combination with the leading inviscid solution should be of a similar order to that estimated above in §4 for the discontinuous case. In particular, for a shear layer of strength $O(\epsilon E^{1/2}/\delta)$ and width $O(\delta)$ interacting with the interior flow of $O(\epsilon)$, we could reasonably expect a torque of $O(\epsilon \times \epsilon E^{1/2}/\delta \times \delta = \epsilon^2 E^{1/2})$ which is sufficient again to drive an $O(\epsilon^2)$ mean flow. As discussed previously, there should not be any loss in order due to phase incoherence between the velocity fields as there was in the shear layer self-interaction case. This is because the initial conditions for the shear layer originate in the viscous boundary layer, where for instance there is certainly no phase coherence between the Ekman efflux velocity and the inviscid interior flow. It is also worth re-emphasizing that large local stresses of $O(\epsilon^2 E^{1/2}/\delta^2)$ seem to be available in the shear layers but, as argued above, have no significance as far as the mean flow is concerned.

Furthermore, the torques produced by shear layers originating from boundary layer eruptions above and below the equator reinforce each other. The linearization of the Navier–Stokes equation ensures that the viscous boundary layer correction, $\tilde{\boldsymbol{u}}_0$, and hence the shear layer velocities $\boldsymbol{u}_s$, shares the equatorial symmetry or antisymmetry of the inviscid inertial wave $\boldsymbol{u}_0$. The azimuthal component of the Reynolds stresses originating from the nonlinear interaction $\boldsymbol{u}_0 \cdot \nabla \boldsymbol{u}_s + \boldsymbol{u}_s \cdot \nabla \boldsymbol{u}_0$ is then symmetric about the equator.

6. Discussion

In this paper, we have argued that the 'eruptions', generic to the Ekman boundary layer associated with any inertial wave, spawn internal shear layers. The presence of these internal shear layers threading through the fluid interior appears to challenge the usual $E^{1/2}$ viscous expansion of the velocity field in a wide variety of situations. Rather than the flow domain being divided into a boundary layer region and an interior with the flow partitioned into $O(\epsilon)$ and $O(\epsilon E^{1/2})$ velocities (ϵ being the Rossby number), there is the possibility of intermediate scales both in the shear layers themselves and at the junctions of these layers with the Ekman boundary layers. Even leaving aside the last possibility, we are forced to contemplate a general expansion of the form

$$\boldsymbol{u} = \epsilon[\boldsymbol{u}_0 + \tilde{\boldsymbol{u}}_0 + E^{1/6}\,\boldsymbol{u}_s^t + E^{3/10}\,\boldsymbol{u}_s^n + E^{1/2}(\boldsymbol{u}_1 + \tilde{\boldsymbol{u}}_1) + o(E^{1/2})] + O(\epsilon^2) \tag{6.1}$$

for the viscous velocity field due to an inertial wave, where velocities with a tilde are only significant in the boundary layer, $\boldsymbol{u}_s^t$ is non-zero only in the shear layer originally tangential to the boundary layer eruption and $\boldsymbol{u}_s^n$ is non-zero in the non-tangential shear layer directed inwards from the boundary layer eruption. Moreover, locating these enlarged viscous velocity fields is in general a non-trivial task. After their initiation at the critical latitudes, the shear layers 'bounce' around off the boundaries always maintaining an inclination of $\tan^{-1}\lambda/(4-\lambda^2)^{1/2}$ to the rotation axis until they eventually dissipate. As a result, their location depends crucially on the global geometry of the container. Walton (1975*a*) talks about an $O(E^{1/6})$ total loss of flux occurring at each reflection in his model problem. This would suggest that a shear layer can survive for at most $O(E^{-1/6})$ traversals of the interior, bearing in mind the further continual viscous attenuation they suffer.

The new shear layer velocities, $\boldsymbol{u}_s^t$ and $\boldsymbol{u}_s^n$, in the expansion (6.1) do not seem important for calculating the viscous frequency shift for the inertial wave. However, they do offer up new possibilities for nonlinear interactions in the interior which, for instance, appear to contribute at leading order to the mean flow. This is because the magnification factor for the shear layer velocities precisely offsets their localization. We have shown how these shear layers can carry angular momentum on their own, but this emerges to be secondary to the transport available in combination with the leading inviscid flow.

An experimental configuration which allows the conclusions reached here to be directly assessed is the slow precession of a spinning oblate spheroid of fluid. If the precession is slow enough, the fluid reacts by tilting its rotation vector away from the spheroid's axis towards the precessional axis (Poincaré 1910). In the container's spinning frame, this response is merely the sustenance of a special 'spinover' inertial wave, which represents a rotation of the fluid about an equatorial axis, at a constant amplitude. As this inertial wave is also a nonlinear solution to the Navier–Stokes equation for all but the non-slip boundary conditions, any discrepancies between this and the observed flow must originate in the Ekman boundary layer necessarily present.

Busse (1968) has already shown how a shear layer in the mean flow observed by Malkus (1968, figure 3) may be generated by nonlinear effects in the Ekman boundary layer. Specifically, Busse found that if the critical latitude singularity in the linearized Ekman boundary layer were retained, it would drive through the nonlinearity a steady mean flow shear layer at the critical radius. However, recent experiments conducted by Vanyo *et al.* (1992, 1995) have highlighted the presence of mean flow shears *throughout* the bulk of the flow. This paper can offer arguments which extend Busse's work to bridge this gap.

Essentially, we suggest that rather than the boundary layer eruptions having influence only locally at the critical radius, they in fact affect the entire flow through obliquely inclined oscillatory shear layers. Since the spinover inertial wave has the same frequency as the basic spin rate of the container, $\lambda = 1$, the boundary layer eruptions occur at any part of the boundary orientated at 30° to the spin axis. The resultant shear layers are then similarly inclined at 30° to the spin axis and therefore penetrate the

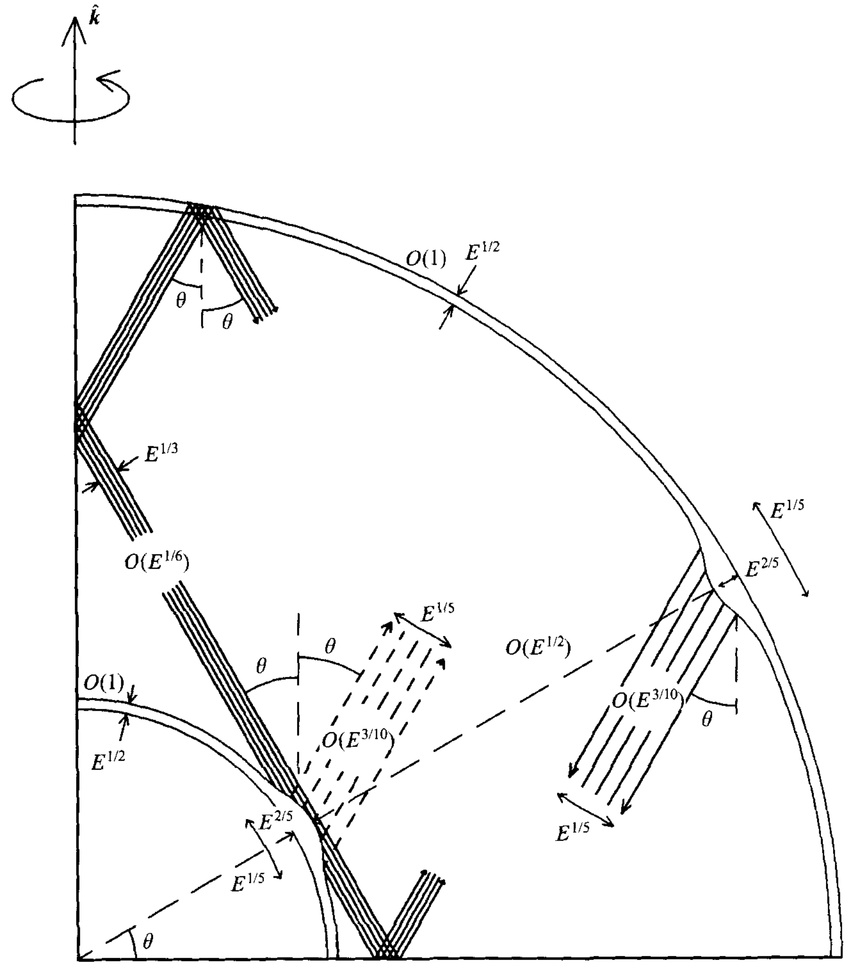

FIGURE 1. A diagram of the viscous response to a spinover velocity field in a spherical shell. The magnitude of the velocity field in each domain, normalized by the basic inviscid spinover amplitude, is shown in orders of the Ekman number; hence the background velocity field is $O(E^{1/2})$. Numerical calculations (Hollerbach & Kerswell 1995) suggest that the inner-core non-tangential shear layer is suppressed; therefore it is only shown dashed. For the spherical case, only the outer weak shear layer is present. $\theta = \tan^{-1}[\lambda/(4-\lambda^2)^{1/2}]$.

entire bulk of the flow. Figure 1 illustrates the situation for a spherical shell where both types of shear layer should be present. In fact, an accompanying numerical calculation of this situation (Hollerbach & Kerswell 1995) indicates that once a tangential shear layer is spawned, the non-tangential shear layer does not appear: presumably, the former sufficiently smooths over the eruption to make the latter redundant.

For the laboratory case of a slightly oblate spheroid, only the non-tangential shear layer appears from the outer eruption. This could not be included in Busse's analysis but has potentially as much influence on the mean flow as the nonlinear boundary layer effects. The selective emanation of the oscillatory shear layer inwards towards the spin axis should in itself set up a mean flow shear layer at the critical radius. Outside the critical radius, the flow is devoid of any shear layers except perhaps the weakened remnant of many reflections. Inside, the newly born shear layer is at the height of its strength to interact with the spinover flow field to despin the fluid. Nowhere else is the contrast so stark. Presumably both the shear layer and nonlinear boundary layer effects conspire to set up the strongest mean flow shear layer precisely at the critical radius. In addition, however, rather than just this one shear layer, we can anticipate that the steadily attenuating oscillatory shear layers bouncing around the interior should produce weaker shears throughout as seemingly observed by Vanyo *et al.* (1995).

Unfortunately, the extra torques available and the resulting driven mean flow cannot be quantified without actually knowing the structure of the shear layers which emanate from the boundary layer eruptions. It perhaps goes without saying that a resolution of the join region where these shear layers emerge from the boundary layer appears well beyond reach and with it any appreciation of the exact structure of the shear layers. Most notably, Moore & Saffman (1969) attempted to fit a steady Stewartson layer onto the Ekman layer encompassing a rising object, but were forced to approach the problem indirectly. Here, the problem is more involved still due to the unsteadiness of the layer and the structure of the boundary layer eruptions. The balance of physical processes which determines the unsteady shear layer is more subtle than that for the steady layer. From (2.5) we have

$$\mathscr{L}[p] = \left\{\frac{\partial^2}{\partial t^2}\nabla^2 + 4\frac{\partial^2}{\partial z^2} - 2E\frac{\partial}{\partial t}\nabla^4 + E^2\nabla^6\right\}p = 0. \tag{6.2}$$

The steady shear layer follows from the leading balance of the second and fourth terms, whereas the unsteady shear layer arises from the third term balancing the residue from the oscillatory balance between the first and second. In terms of the characteristic variables

$$\sigma_\pm = s \pm \frac{\lambda}{(4-\lambda^2)^{1/2}}z \tag{6.3}$$

(6.2) is to leading order

$$\left\{4\frac{\partial^2}{\partial\sigma_\pm\,\partial\sigma_\mp} + \frac{1}{s}\frac{\partial}{\partial\sigma_\pm} + \frac{32iE}{\lambda(4-\lambda^2)^2}\frac{\partial^4}{\partial\sigma_\pm^4}\right\}p \sim 0 \tag{6.4}$$

along a $\sigma_\pm$ = constant shear layer. The absence of the highest derivative from this leading balance has been noted before (Wood 1966; Walton 1975*a*, *b*). If the shear layer scales with $E^{1/3}$, all three terms are comparable. If the shear layer is weaker, only the first two balance.

The conclusions drawn here can to some extent be confirmed through comparison with a full numerical solution of the viscous correction to the spinover inertial wave in a sphere and spherical shell. This work is described in an accompanying paper (Hollerbach & Kerswell 1995). The associated driven mean flow exhibits shear throughout the interior as expected.

Appendix

In the resonant case $\lambda = 2$, the roots of (2.11) are

$$\left.\begin{aligned}\alpha_1 &= E^{-1/4}k^{1/2}\mathrm{e}^{-\mathrm{i}\pi/8} + O(E^{3/4}k^{5/2}),\\ \alpha_2 &= E^{-1/4}k^{1/2}\mathrm{e}^{3\mathrm{i}\pi/8} + O(E^{3/4}k^{5/2}),\\ \alpha_3^2 &= 4\mathrm{i}E^{-1} + 5k^2/4 + O(Ek^4),\end{aligned}\right\} \tag{A 1}$$

where now only α_3 is associated with the Ekman boundary layer. Eliminating A_3 from the boundary conditions (3.3) and (3.4) gives

$$\frac{A_1}{\sinh(\alpha_2 d)} \approx -\frac{A_2}{\sinh(\alpha_1 d)} \approx \frac{E\alpha_1^3 J_m(k)}{k[\cosh(\alpha_1 d)\sinh(\alpha_2 d) - \mathrm{i}\sinh(\alpha_1 d)\cosh(\alpha_2 d)]} \tag{A 2}$$

and the solution

$$u-\mathrm{i}v \approx -2\mathrm{i}\epsilon\,\mathrm{e}^{\mathrm{i}(m\phi+2t)}\int_0^\infty \mathrm{d}k\, J_m(k)\, J_{m-1}(ks) \times\left[\frac{\cosh(\alpha_1 z)\sinh(\alpha_2 d)-\mathrm{i}\sinh(\alpha_1 d)\cosh(\alpha_2 z)}{\cosh(\alpha_1 d)\sinh(\alpha_2 d)-\mathrm{i}\sinh(\alpha_1 d)\cosh(\alpha_2 d)}\right] \quad \text{(A 3)}$$

valid away from the Ekman boundary layer. The integrand is significant only up to wavenumbers $k \sim O(E^{1/2}/\Delta^2)$ where $\Delta = d-|z| \gg E^{1/2}$ and hence this solution possesses a boundary layer structure of its own with thickness $E^{1/4}$. Letting $x = \Delta E^{-1/4} k^{1/2}$ and taking $\Delta \ll 1$ to simplify the integrand, the solution is

$$u-\mathrm{i}v \sim -2(1+\mathrm{i})\frac{\epsilon E^{1/2}}{\Delta^2}\mathrm{e}^{\mathrm{i}(m\phi+2t)}\int_0^\infty x\,\mathrm{d}x\, J_m\!\left(\frac{E^{1/2}}{\Delta^2}x^2\right) J_{m-1}\!\left(\frac{E^{1/2}}{\Delta^2}sx^2\right) \times[\mathrm{i}\exp(-x\,\mathrm{e}^{-\mathrm{i}\pi/8})-\exp(-x\,\mathrm{e}^{3\mathrm{i}\pi/8})]. \quad \text{(A 4)}$$

The magnitude of the velocity field falls off from $O(\epsilon)$ inside the $E^{1/4}$ layer to

$$u-\mathrm{i}v \sim O(\epsilon[E^{1/2}/\Delta^2]^{m+1+|m-1|}), \quad \text{(A 5)}$$

which holds for the interior $d-|z| \sim O(1)$ as well.

This confirms the scaling predictions of Gans (1983) who foresaw the possibility of an $E^{1/2}$ layer embedded in an $E^{1/4}$ layer for the special resonant case where a plane boundary is perpendicular to the rotation axis. Gans found that an $E^{1/3}$ layer could also exist for all other orientations. In effect, the extra $E^{1/4}$ boundary layer represents the limiting case of a horizontal shear layer arising from the boundary discontinuity. In contrast, an associated but subtly different problem of a resonantly oscillating, infinite disk (Benney 1965; Thornley 1968), or pair of disks (Barrett 1969; Jacobs 1971), does not contain an $E^{1/4}$ layer.

REFERENCES

BARRETT, K. E. 1969 Resonant torsional oscillations of a pair of discs in a rotating fluid. *Z. Angew. Math. Phys.* **20**, 721–729.

BENNEY, D. J. 1965 The flow induced by a disk oscillating about a state of steady rotation. *Q. J. Mech. Appl. Maths* **18**, 333–345.

BONDI, H. & LYTTLETON, R. A. 1953 On the dynamical theory of the rotation of the Earth: the effect of precession on the motion of the liquid core. *Proc. Camb. Phil. Soc.* **49**, 498.

BUSSE, F. H. 1968 Steady fluid flow in a precessing spheroidal shell. *J. Fluid Mech.* **33**, 739–751.

GANS, R. F. 1983 Boundary layers on characteristic surfaces for time-dependent rotating flows. *Trans. ASME* E: *J. Appl. Mech.* **50**, 251–254.

GÖRTLER, H. 1944 Einige Bemerkungen über Strömungen in rotierenden Flüssigkeiten. *Z. Angew. Math. Mech.* **24**, 210–214.

GÖRTLER, H. 1957 On forced oscillations in rotating fluids. *5th Midwestern Conf. on Fluid Mech.*, pp. 1–10.

GREENSPAN, H. P. 1964 On the transient motion of a contained rotating fluid. *J. Fluid Mech.* **20**, 673–696.

GREENSPAN, H. P. 1965 On the general theory of contained rotating fluid motions. *J. Fluid Mech.* **22**, 449–462.

GREENSPAN, H. P. 1968 *The Theory of Rotating Fluids.* Cambridge University Press; reprinted Breukelen Press, Brookline (1990).

GREENSPAN, H. P. & HOWARD, L. N. 1963 On a time dependent motion of a rotating fluid. *J. Fluid Mech.* **17**, 385–404.

HOLLERBACH, R. & KERSWELL, R. R. 1995 Oscillatory internal shear layers in rotating and precessing flows. *J. Fluid Mech.* **298**, 327–339.

JACOBS, C. 1971 Transient motions produced by disks oscillating torsionally about a state of rigid rotation. *Q. J. Mech. Appl. Maths* **24**, 221–236.

JACOBS, S. J. 1964 The Taylor column problem. *J. Fluid Mech.* **20**, 581–591.

KERSWELL, R. R. 1994 Tidal excitation of hydromagnetic waves and their damping in the Earth. *J. Fluid Mech.* **274**, 219–241.

KERSWELL, R. R. & BARENGHI, C. F. 1995 On the viscous decay rates of inertial waves in a rotating circular cylinder. *J. Fluid Mech.* **285**, 203–214.

MALKUS, W. V. R. 1968 Precession of the Earth as the cause of geomagnetism. *Science* **169**, 259–264.

MCEWAN, A. D. 1970 Inertial oscillations in a rotating fluid cylinder. *J. Fluid Mech.* **40**, 603–640.

MOORE, D. W. & SAFFMAN, P. G. 1969 The structure of free vertical shear layers in a rotating fluid and the motion produced by a slowly rising body. *Phil. Trans. R. Soc. Lond.* A **264**, 597–634.

MORRISON, J. A. & MORGAN, G. W. 1956 The slow motion of a disc along the axis if a viscous rotating fluid. *Tech. Rep. Div. Appl. Math., Brown University*, vol. 8.

OSER, H. 1957 Erzwungene Schwingungen in rotierenden Flussigkeiten. *Arch. Rat. Mech. Anal.* **1**, 81–96.

OSER, H. 1958 Experimentelle Untersuchung uber harmonische Schwingungen in rotierenden Flussigkeiten. *Z. angew. Math. Mech.* **38**, 386–391.

PHILLIPS, O. M. 1963 Energy transfer in rotating fluids by reflection of inertial waves. *Phys. Fluids* **6**, 513–520.

POINCARÉ, H. 1910 Sur la précession des corps deformable. *Bull. Astron.* **27**, 321.

PROUDMAN, I. 1956 The almost-rigid rotation of viscous fluid between concentric spheres. *J. Fluid Mech.* **1**, 505–516.

REYNOLDS, A. 1962*a* Forced oscillations in a rotating liquid (I). *Z. angew. Math. Phys.* **13**, 460–468.

REYNOLDS, A. 1962*b* Forced oscillations in a rotating liquid (II). *Z. angew. Math. Phys.* **13**, 561–572.

ROBERTS, P. H. & STEWARTSON, K. 1963 On the stability of a Maclaurin spheroid of small viscosity. *Astrophys. J.* **137**, 777–790.

SNEDDON, I. N. 1951 *Fourier Transforms*. McGraw-Hill.

STEWARTSON, K. 1957 On almost rigid rotations. *J. Fluid Mech.* **3**, 17–26.

STEWARTSON, K. 1966 On almost rigid rotations. Part 2. *J. Fluid Mech.* **26**, 131–144.

THORNLEY, C. 1968 On Stokes and Rayleigh layers in a rotating system. *Q. J. Mech. Appl. Maths* **21**, 451–461.

VANYO, J. P., WILDE, P., CARDIN, P. & OLSON, P. 1992 Flow structures induced in the liquid core by precession. *Abstract AGU EOS* **73**, 63 (Supplement).

VANYO, J. P., WILDE, P., CARDIN, P. & OLSON, P. 1995 Experiments on precessing flows in the Earth's liquid core. *Geophys. J. Intl* **121**, 136–142.

WALTON, I. C. 1975*a* Viscous shear layers in an oscillating rotating fluid. *Proc. R. Soc. Lond.* A **344**, 101–110.

WALTON, I. C. 1975*b* On waves in a thin rotating spherical shell of slightly viscous fluid. *Mathematika* **22**, 46–59.

WOOD, W. W. 1965 Properties of inviscid, recirculating flows. *J. Fluid Mech.* **22**, 337–346.

WOOD, W. W. 1966 An oscillatory disturbance of rigidly rotating fluid. *Proc. R. Soc. Lond.* A **298**, 181–212.

WOOD, W. W. 1977 Inertial oscillations in a rigid axisymmetric container. *Proc. R. Soc. Lond.* A **358**, 17–30.

WOOD, W. W. 1981 Inertial modes with large azimuthal wavenumbers in an axisymmetric container. *J. Fluid Mech.* **105**, 427–449.